

Figure 1. ESR spectrum of the ScCO molecule in an argon matrix at 4 K showing the eight ^{45}Sc ($I = 7/2$) hyperfine lines on a varying background ($\nu = 9.5792$ GHz).

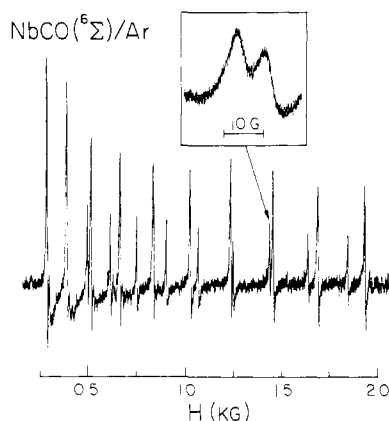


Figure 2. ESR spectrum of the NbCO molecule in an argon matrix at 4 K. The two series of ten lines are due to hyperfine interaction with the ^{93}Nb ($I = 9/2$) nucleus. Each line of the weak series is split by 6.6 G by introduction of ^{13}C , as shown in the inset, and is therefore identified with NbCO. The stronger series is due to an unidentified molecule (see text): ($\nu = 9.5773$ GHz).

unchanged by introduction of ^{13}C in the matrix. They are possibly due to a niobium carbene molecule formed from background hydrocarbon and require further investigation. The procedures for forming the matrices and measuring these spectra were the same as used previously.⁷ The magnetic parameters, obtained in the usual way,^{5,8} are listed in Table I. At least one higher field fine structure transition could also appear in each of these spectra but only if the zero-field-splitting (zfs) parameter $|D|$ is not too large.⁸ Our inability to detect it in each case probably indicates that $|D| \geq 1$ cm⁻¹.

The unpaired spin configuration^{3,4} in ScCO is nominally $s\sigma^1d\pi^2$, but the $s\sigma$ orbital is hybridized with $d\sigma$ and $p\sigma$, and the π electrons are partially $p\pi$ of the metal and $2\pi^*$ of CO. (The negligible ^{13}C hfs indicates very little spin density in the $s\sigma$ orbital on CO.) From ^{45}Sc atomic data⁹ $A_{\text{iso}} = 2823 \times 1/3 = 941$ MHz, and comparison with the value in Table I yields 58% s character at the metal, as given there. The observed $A_{\text{dip}}(^{45}\text{Sc}) = +58 \pm 11$ MHz suggests that this value may be too high since a large contribution of $4p\sigma$ and perhaps $d\sigma$ character, which contribute positively to the anisotropic hf, would appear to be required. For example, the configuration $(s\sigma^{0.58} + p\sigma^{0.42})d\pi^2$ yields a value of $A_{\text{dip}} \cong +36$ MHz, and placing spin in the $2\pi^*$ orbital would lower this value further. These approximate deductions are not in agreement with theoretical calculations⁴ which predict a considerably higher % s character.

(7) Van Zee, R. J.; Baumann, C. A.; Weltner, W., Jr. *J. Chem. Phys.* **1985**, *82*, 3912-20. Van Zee, R. J.; Ferrante, R. F.; Zeringue, K. J.; Weltner, W., Jr. *J. Chem. Phys.* **1988**, *88*, 3465-74.

(8) Weltner, W., Jr. *Magnetic Atoms and Molecules*; Van Nostrand Reinhold: New York, 1983.

(9) Morton, J. R.; Preston, K. F. *J. Magn. Reson.* **1978**, *30*, 577-582.

Table I. Derived Magnetic Parameters for $^{45}\text{Sc}^{13}\text{CO}(^4\Sigma)$ and $^{93}\text{Nb}^{13}\text{CO}(^6\Sigma)$ in Solid Argon at 4 K

	$^{45}\text{Sc}^{13}\text{CO}$	$^{93}\text{Nb}^{13}\text{CO}$
g_{\parallel}	2.0023 ^a	2.0023 ^a
g_{\perp}	1.772 (4)	1.980 (2)
$ D $ (cm ⁻¹)	≥ 1.0	≥ 1.0
$ A_{\parallel} ^b$ (MHz)	658 (30)	420 (30)
$ A_{\perp} ^b$ (MHz)	483 (2)	442 (1)
$A_{\text{iso}}^{b,c}$ (MHz)	541 (11)	434 (13)
$A_{\text{dip}}^{b,c}$ (MHz)	58 (11)	-7 (12)
$ \psi(0) ^2$ ^b (au)	0.497 (10)	0.40 (1)
$((3 \cos^2 \theta - 1)/r^3)^b$ (au)	0.89 (7)	0.11 (19)
% s character on metal	58	33
$ A_{\perp}(^{13}\text{C}) $ (MHz)	<4	16 (2)

^a Assumed. ^b At metal nucleus. ^c Assuming A_{\perp} and A_{\parallel} are positive in sign.

The large negative value of $\Delta g_{\perp} = g_{\perp} - g_e = -0.23$ found for ScCO indicates that a low-lying $^4\Pi(s\sigma^1d\pi^1d\delta^1)$ state is coupled to the $X^4\Sigma$. This is in general accord with the ab initio calculations which place such a state at ~ 3000 cm⁻¹.^{3,4} From Δg_{\perp} , assuming an average spin-orbit coupling constant of 60 cm⁻¹¹⁰ and a simple $d\pi \rightarrow d\delta$ excitation, we find $\Delta E \cong 500$ cm⁻¹!

NbCO appears to be like VCO in all respects except that the value of $|D| \geq 1$, and this is presumably related to the higher spin-orbit coupling constant of Nb relative to V (480 vs 150 cm⁻¹). The % s character on the metals are quite close, 33 vs $\sim 27\%$; A_{dip} values are -7(12) vs $\sim -10(8)$ MHz, and the ^{13}C splittings are both about 6 G. The analyses of the ESR results are then much the same and imply that the electronic structures of $^6\Sigma$ VCO and NbCO are surprisingly similar.

Since several theoretical calculations have indicated that the lowest states of the FeCO molecule are $^3\Sigma$ and $^5\Sigma$, the nonobservance of an ESR spectrum is attributed here to a zfs parameter $|D| \geq 2$ cm⁻¹. This is reasonable in comparison with ScCO and VCO since $|D|$ varies roughly as the square of the spin-orbit coupling constant.

Acknowledgment. This research was supported by the National Science Foundation (Grant CHE-8814297).

(10) Dunn, T. M. *Trans. Faraday Soc.* **1961**, *57*, 1441-1444.

Shape-Selective Targeting of DNA by (Phenanthrenequinone diimine)rhodium(III) Photocleaving Agents

Anna Marie Pyle, Eric C. Long, and Jacqueline K. Barton*

Department of Chemistry, Columbia University
New York, New York 10027

Received December 16, 1988

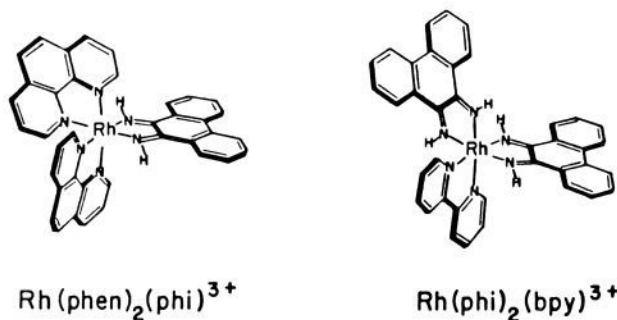
There has been considerable interest in the design of molecules which recognize and react at DNA sites in a sequence-defined fashion.^{1,2} We report here the design of a family of new, highly efficient, photocleaving molecules which appear to recognize ostensibly B-form DNA sites on the basis of considerations of shape. Phenanthrenequinone diimine (phi) complexes³ of rho-

(1) Dervan, P. B. *Nucleic Acids Mol. Biol.* **1988**, *2*, 49. Moser, H. E.; Dervan, P. *Science* **1987**, *238*, 645. Chen, C.-H. B.; Sigman, D. S. *Science* **1987**, *217*, 1197. Hecht, S. M. *Acc. Chem. Res.* **1986**, *19*, 383.

(2) Barton, J. K. *Science* **1986**, *233*, 727. Fleisher, M. B.; Mei, H.-Y.; Barton, J. K. *Nucleic Acids Mol. Biol.* **1988**, *2*, 65. Mei, H.-Y.; Barton, J. K. *Proc. Natl. Acad. Sci. U.S.A.* **1988**, *85*, 1339. Kirshenbaum, M. R.; Tribollet, R.; Barton, J. K. *Nucleic Acids Res.* **1988**, *16*, 7943.

(3) The syntheses and characterizations of [Rh(phen)phi]Cl₃ and [Rh(phi)phi]Cl₃ are available as Supplementary Material. Full details will be provided in a subsequent publication.

dium(III) were selected for these studies so as to maximize DNA binding affinity⁴ and photocleavage efficiency.^{5,6} Upon photoactivation, the complex bis(phenanthroline)(9,10-phenanthrenequinone diimine)rhodium(III), $\text{Rh}(\text{phen})_2\text{phi}^{3+}$, cleaves double-stranded DNA selectively at 5'-pyrimidine-purine-3' steps and in particular at the consensus sequence 5'-CCAG-3', while the analogue bis(phenanthrenequinone diimine)(bipyridyl)rhodium(III), $\text{Rh}(\text{phi})_2(\text{bpy})^{3+}$, despite containing ancillary imines for potential hydrogen bonding, cleaves DNA efficiently but in a generally sequence-neutral fashion.



$\text{Rh}(\text{phen})_2\text{phi}^{3+}$ and $\text{Rh}(\text{phi})_2\text{bpy}^{3+}$ cleave supercoiled DNA efficiently upon photoactivation (310–356 nm) to produce nicked form II DNA. Without irradiation, DNA cleavage is not observed in the presence of metal complex. Figure 1A shows the results of photocleavage of ³²P-end-labeled linear DNA restriction fragments. $\text{Rh}(\text{phen})_2\text{phi}^{3+}$ and $\text{Rh}(\text{phi})_2\text{bpy}^{3+}$ display different patterns of cleavage, despite their overall similarities in coordination geometry and ligands. $\text{Rh}(\text{phen})_2\text{phi}^{3+}$ cleaves at single base positions on each of the two strands primarily at sites containing the sequence 5'-CCAG-3'.⁷ The single site cleavage patterns suggest the absence of a diffusible species mediating the strand scission. The asymmetry in cleavage pattern at a site to the 5'-side on each strand points to cleavage by the rigid complex from the major groove of the helix.⁸ This result represents a first demonstration of such cleavage of B-DNA from the major groove for a small molecule. In contrast to these site-selective cleavage patterns, little sequence selectivity is apparent with $\text{Rh}(\text{phi})_2\text{bpy}^{3+}$.⁹

The difference in DNA photocleavage selectivities of these complexes does not appear to depend upon differences in their mechanism of strand scission. Upon photoactivation, $\text{Rh}(\text{phen})_2\text{phi}^{3+}$ and $\text{Rh}(\text{phi})_2(\text{bpy})^{3+}$ mediate the release of nucleic acid bases (Figure 1B) and the formation of 5'- and 3'-phosphate termini (data not shown),² suggesting the sugar as the site of reaction.¹⁰

The differences in site selectivities appear to depend instead upon differences in DNA binding characteristics. Given the propensity of the phi ligand for intercalation,⁴ we expect that in the DNA-bound form, $\text{Rh}(\text{phen})_2\text{phi}^{3+}$ would contain the phenanthroline ligands in ancillary, nonintercalative positions along

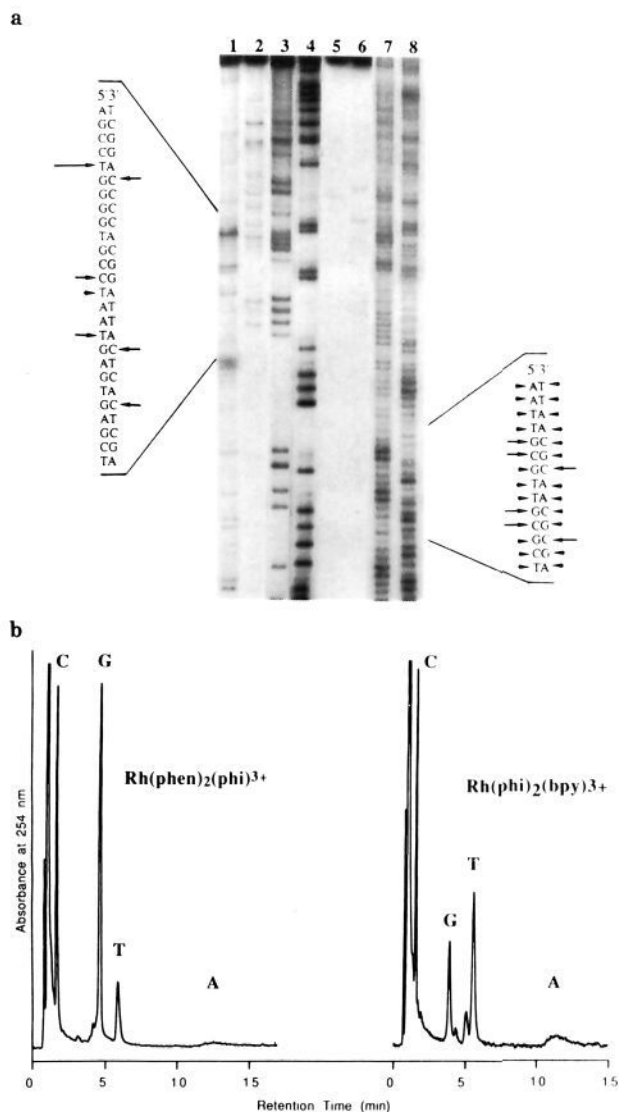


Figure 1. Products of photocleavage by $\text{Rh}(\text{phen})_2(\text{phi})^{3+}$ and $\text{Rh}(\text{phi})_2(\text{bpy})^{3+}$. **A.** Autoradiogram of a high resolution polyacrylamide gel of linear DNA fragments after photocleavage. Cleavage is shown on the 3'- and 5'-end-labeled strands of a 230 base-pair DNA restriction fragment (PvuII \rightarrow HindIII) from the pUC18 plasmid. Lanes 1 and 2: $\text{Rh}(\text{phen})_2(\text{phi})^{3+}$ photocleavage products on the 3'- and 5'-labeled strands, respectively. Irradiations were at 356 nm for 1 min. Lanes 3 and 4: Maxam-Gilbert guanine-specific reactions on the 3'- and 5'-labeled strands, respectively. Lane 5: 3'-labeled strand light control, irradiation at 356 nm for 7 min without metal complex. Lane 6: 5'-labeled strand light control, irradiation at 310 nm for 7 min. Lanes 7 and 8: photocleavage by $\text{Rh}(\text{phi})_2(\text{bpy})^{3+}$ on the 3'- and 5'-labeled strands, respectively, with irradiation at 310 nm for 3 min. Irradiations were performed using a 1000 W Hg/Xe lamp and monochromator in 20 μL volumes containing 50 μM DNA and 5 μM rhodium complex in 50 mM Tris, 20 mM NaAcetate, 18 mM NaCl, pH 7. Patterns of cleavage were not found to be wavelength dependent. **B.** HPLC chromatograms of calf thymus DNA cleavage products after irradiation in the presence of $\text{Rh}(\text{phen})_2(\text{phi})^{3+}$ (left) and $\text{Rh}(\text{phi})_2(\text{bpy})^{3+}$ (right). Cleavage reactions were performed in 40 μL volume containing 500 μM calf thymus DNA-nucleotide, 200 μM Rh, and 50 mM Na-cacodylate buffer, pH 7.0. Samples were irradiated at 310 nm for 10 min ($\text{Rh}(\text{phen})_2\text{phi}^{3+}$) or 50 min ($\text{Rh}(\text{phi})_2\text{bpy}^{3+}$) followed by reverse phase HPLC analysis on a Rainin Microsorb "Short-One" C-18 column (3 μ) eluted with 0.1 M ammonium formate, pH 7.0. Products were detected at 254 nm.

(4) Pyle, A. M.; Rehmann, J. P.; Meshoyrer, R.; Kumar, C. V.; Turro, N. J.; Barton, J. K. *J. Am. Chem. Soc.* **1989**, *111*, 3051.

(5) Chan, S.-F.; Chou, M.; Creutz, C.; Matsubara, T.; Sutin, N. *J. Am. Chem. Soc.* **1981**, *103*, 369. Indelli, M. T.; Carioli, A.; Scandola, F. *J. Phys. Chem.* **1984**, *88*, 2685. Ohno, T. *Coord. Chem. Rev.* **1985**, *64*, 311.

(6) Only one synthesis of phi complexes of rhodium has been reported. See: Schlosser, v. K. Z. *Anorg. Allg. Chem.* **1972**, *387*, 91. For spectroscopic studies of ruthenium complexes of phi, see: Pyle, A. M.; Barton, J. K. *Inorg. Chem.* **1987**, *26*, 3820. Belser, P.; von Zelewsky, A.; Zehnder, M. *Inorg. Chem.* **1981**, *20*, 1098.

(7) Cleavage is found also at the sequences 5'-CCAA-3', 5'-TCGT-3', and 5'-TCAT-3' though with lower intensity. These site selectivities have been determined with the racemic complexes.

(8) Dervan, P. B. *Science* **1986**, *232*, 464.

(9) At short irradiation times, some sequence preference is evident at 5'-TGCGT-3', 5'-TGCGC-3', 5'-TGCC-3', and 5'-TGCCT-3'. The asymmetry in cleavage pattern at these sites also indicates access from the major groove.

(10) For an excellent discussion of routes for DNA cleavage, see: Stubbe, J.; Kozarich, J. W. *Chem. Rev.* **1987**, *87*, 1107.

the groove, while for $\text{Rh}(\text{phi})_2\text{bpy}^{3+}$, one phi and one bpy would occupy the ancillary sites. For $\text{Rh}(\text{phi})_2\text{bpy}^{3+}$, based upon inspection of models, the ancillary phi ligand could be well-positioned for hydrogen bonding of the imine proton to the guanine O6 oxygen atom; no hydrogen bonding possibilities exist for the in-

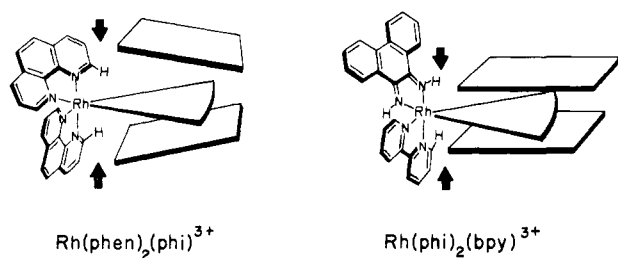


Figure 2. Matching the rhodium complex shapes to those of DNA sites. The schematic illustrates intercalation of $\text{Rh}(\text{phen})_2(\text{phi})^{3+}$ (left) and $\text{Rh}(\text{phi})_2(\text{bpy})^{3+}$ (right) into either an opened or canonical major groove site, respectively. For $\text{Rh}(\text{phen})_2(\text{phi})^{3+}$, the potential steric clashes between ancillary ligand hydrogen atoms and the base pair planes lead to the accommodation of the complex preferentially at such opened sites, whereas $\text{Rh}(\text{phi})_2(\text{bpy})^{3+}$, with recessed ancillary ligands, fits easily into the canonical intercalation site.

tercalated $\text{Rh}(\text{phen})_2(\text{phi})^{3+}$. The sequence selectivities found here do not appear to be dominated by such hydrogen bonding considerations, however, since it is the complex lacking hydrogen bonding groups in ancillary positions that shows the greater sequence selectivity.¹¹ Instead the sequence selectivity observed must depend upon steric factors and a complementarity of the shape of the metal complex to the local conformation of the DNA site. Figure 2 illustrates a model which rationalizes the different site selectivities observed. In B-DNA, at 5'-pyrimidine-purine-3' base steps, propeller twisting leads to steric clashes between the cross strand purine bases in the minor groove with a concomitant opening of the major groove.^{12,13} The sequences cleaved preferentially by $\text{Rh}(\text{phen})_2(\text{phi})^{3+}$ are those which show the largest extent of such a major groove opening.^{14,15} With the phi ligand inserted deeply between the base pairs, $\text{Rh}(\text{phen})_2(\text{phi})^{3+}$ appears to require sites with a more opened major groove; otherwise steric clashes may ensue between bases above and below the intercalation site and the overhanging phenanthroline H2 and H9 hydrogen atoms. For $\text{Rh}(\text{phi})_2(\text{bpy})^{3+}$, in contrast, the ancillary ligands do not overhang the metal center, and only the potentially hydrogen bonding imine protons about the helical groove. Substantive intercalation by $\text{Rh}(\text{phi})_2(\text{bpy})^{3+}$ from the major groove, therefore, appears possible at all sites along the helix.

Rhodium(III) complexes of the phi ligand and its derivatives provide efficient photocleaving reagents, and they may find application both in vitro and in vivo. $\text{Rh}(\text{phen})_2(\text{phi})^{3+}$ becomes in particular a useful probe of the local variations in major groove size. Furthermore these results underscore the importance of considerations of shape in the design of sequence-specific molecules targeted to DNA.¹⁶

Acknowledgment. We are grateful to the NIH (GM33309 to J.K.B.; National Research Service Training Award for A.M.P., GM07216) and to the NSF for their financial support.

Supplementary Material Available: Synthesis and characterization data (NMR, FABMS, and UV-vis) for $[\text{Rh}(\text{phen})_2(\text{phi})\text{Cl}_3]$ and $[\text{Rh}(\text{phi})_2(\text{bpy})\text{Cl}_3]$ (2 pages). Ordering information is given on any current masthead page.

(11) The weak selectivity of $\text{Rh}(\text{phi})_2(\text{bpy})^{3+}$ for the 5'-TGC-3' site may be related to such hydrogen bonding interactions.

(12) Calladine, C. R. *J. Mol. Biol.* **1982**, *161*, 343.

(13) Dickerson, R. E. *J. Mol. Biol.* **1983**, *166*, 419.

(14) Nelson, H. C. M.; Finch, J. T.; Luisi, B. F.; Klug, A. *Nature* **1987**, *330*, 221. Satchwell, S. C.; Drew, H. R.; Travers, A. A. *J. Mol. Biol.* **1986**, *191*, 659.

(15) Intercalation may alter these conformational effects, although the stacking of phi between the base pairs could serve to reinforce the purine-purine stacking and roll.

(16) Recent crystal structures of protein-DNA complexes indicate that shape-selection may be an important feature also in the recognition of specific DNA sites by proteins. See, for example: Otwinowski, Z.; Schevitz, R. W.; Zhang, R.-G.; Lawson, C. L.; Joachimiak, A.; Marmorstein, R. Q.; Luisi, B. F.; Sigler, P. B. *Nature* **1988**, *335*, 321.

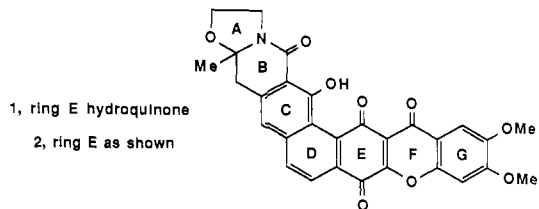
Synthesis of (±)-Cervinomycins A₁ and A₂

T. Ross Kelly,* Christopher T. Jagoe, and Qun Li

Department of Chemistry, Boston College
Chestnut Hill, Massachusetts 02167

Received February 13, 1989

The cervinomycins¹ are recently reported members of a small but growing family² of naturally occurring antibiotics, all of which possess xanthone- and isoquinolone-based units embedded within a larger polycyclic framework. To date, no synthesis of any member of this group has been recorded.³ We now report the synthesis of cervinomycins A₁ (**1**) and A₂ (**2**).



Considerations of synthetic economy dictated a convergent approach to the heptacyclic targets. A sequence based on the union of ABC and EFG fragments in the course of constructing the D ring appeared especially attractive. Preliminary studies indicated that the two extra carbons destined to become the phenanthrene bridge of the D ring could be effectively carried forward as an appendage to the ABC unit (→ ABC_D).

Construction of the EFG portion was straightforward⁴ (Scheme 1). Coupling of **3**⁵ with **4**⁶ proceeds via an addition/elimination mechanism to give **5**. That the reaction occurs with ipso and not cine⁸ substitution of the iodine was established^{4,9} by ¹H NMR (*J*_{AB} = 2.4 Hz). Reduction of **5** to the hydroquinone followed by cyclization⁴ affords **6**. Findings later in the synthesis required

(1) Ōmura, S.; Nakagawa, A.; Kushida, K.; Lukacs, G. *J. Am. Chem. Soc.* **1986**, *108*, 6088-6089. Ōmura, S.; Nakagawa, A.; Kushida, K.; Shimizu, H.; Lukacs, G. *J. Antibiot.* **1987**, *40*, 301-308. For the original isolation, see: Ōmura, S.; Iwai, Y.; Hinotozawa, K.; Takahashi, Y.; Kato, J.; Nakagawa, A.; Hirano, A.; Shimizu, H.; Haneda, K. *J. Antibiot.* **1982**, *35*, 645-652. Qi, C.; Tian, J.; Marunaka, T.; Yamada, Y.; Yamawaki, I.; Ohtani, T.; Minami, Y.; Saito, H. Eur. Pat. Appl. EP 246,091, Nov 19, 1987; *Chem. Abstr.* **1988**, *108*, 130060d. For derivatives, see: Nakagawa, A.; Iwai, Y.; Shimizu, H.; Ōmura, S. *J. Antibiot.* **1986**, *39*, 1636-1638.

(2) Other members of the family include the following: (a) *Lysolipin I*, Dobler, M.; Keller-Schierlein, W. *Helv. Chim. Acta* **1977**, *60*, 178-185. Drautz, H.; Keller-Schierlein, W.; Zähler, H. *Arch. Microbiol.* **1975**, *106*, 175. (b) *Albofungin* and *chloroalbofungin*, for the initial structure assignments, see, inter alia: Gurevich, A. I.; Karapetyan, M. G.; Kolosov, M. N.; Omelchenko, V. N.; Onoprienko, V. V.; Petrenko, G. I.; Popravko, S. A. *Tetrahedron Lett.* **1972**, 1751-1754. Gurevich, A. I.; Deshko, T. N.; Kogan, G. A.; Kolosov, M. N.; Kudryashova, V. V.; Onoprienko, V. V. *Tetrahedron Lett.* **1974**, 2801-2804. A subsequent structure revision appears to have passed largely unnoticed: Onoprienko, V. V.; Kozmin, Y. P.; Kolosov, M. N. *Biorg. Khim.* **1978**, *4*, 1418-1422; *Chem. Abstr.* **1979**, *90*, 54885u. (c) *LL-D42067α* and *LL-D42067β*, Labeda, D. P.; Kantor, S.; Kennett, R. L., Jr.; Carter, G. T.; Lee, T. M.; Borders, D. B.; Goodman, J. J.; Testa, R. T.; Maiese, W. M. U.S. Pat. Appl. 593,160, Mar 26, 1984; *Chem. Abstr.* **1986**, *104*, 62068c. (d) *Actinoplanones A-G*, Kobayashi, K.; Nishino, C.; Ohya, J.; Sato, S.; Mikawa, T.; Shiobara, Y.; Kodama, M. *J. Antibiot.* **1988**, *41*, 502-511, 741-750.

(3) (a) For a summary of model studies directed toward the synthesis of lysolipin I,^{2a} see: Duthaler, R. O.; Heuberger, C.; Wegmann, U. H.-U.; Scherrer, V. *Chimia* **1985**, *39*, 174-182. For model studies relating to the synthesis of the cervinomycins, see: (b) Rama Rao, A. V.; Reddy, K. K.; Yadav, J. S.; Singh, A. K. *Tetrahedron Lett.* **1988**, *29*, 3991-3992. (c) Mehta, G.; Venkateswarlu, Y. *J. Chem. Soc., Chem. Commun.* **1988**, 1200-1202.

(4) Based on the method reported in Brassard, P.; Simoneau, B. *J. Chem. Soc., Perkin Trans. I* **1984**, 1507-1510.

(5) Commercially available from Lancaster Synthesis Ltd.

(6) Prepared in 73% overall yield from 2,4,5-trimethoxybenzoic acid (Aldrich) by selective⁷ monodemethylation with BBr₃ in CH₂Cl₂ and esterification (CH₂N₂). For a lengthier synthesis, see: Hemmelmayr, F. V. *Monatsh. Chem.* **1914**, *35*, 1-8.

(7) Compare: Dean, F. M.; Goodchild, J.; Houghton, L. E.; Martin, J. A.; Morton, R. B.; Parton, B.; Price, A. W.; Somvichien, N. *Tetrahedron Lett.* **1966**, 4153-4159.

(8) For instances of cine substitution of haloquinones, see: Finley, K. T. In *The Chemistry of Quinonoid Compounds*; Patai, S., Ed.; Wiley Interscience: New York, 1974; p 895 and references thereto.